Small-Angle Neutron Scattering Investigation of the *Q*-Dependence of the Flory−Huggins Interaction Parameter in a Binary Polymer Blend

A. Zirkel*,† and S. M. Gruner

Physics Department, Cornell University, 162 Clark Hall, Ithaca, New York 14853-2501

V. Urban‡ and P. Thiyagarajan

Intense Pulsed Neutron Source Divison, Argonne National Laboratory, 9700 South Cass Avenue, Argonne, Illinois 60439

Received April 2, 2001; Revised Manuscript Received June 5, 2002

ABSTRACT: It is usually assumed that the Flory−Huggins interaction parameter χ in polymer blends can be represented by a structureless, pointlike interaction. On a local scale, however, the Flory−Huggins parameter must show a spatial dependence as it basically reflects the segment−segment interaction potential. We show that SANS can be used to access this spatial dependence and that even in the SANS regime, a pronounced Q dependence of χ is found. The polymer blend used in the experiments was a polystyrene/poly(*p*-methylstyrene) blend. As we did not want to rely on literature values for the segment lengths of PS and PPMS, respectively, we measured the isotope blends of h-PS/d-PS and h-PPMS/d-PPMS separately. A modified random phase formula based on the PRISM theory of Schweizer and Chandler is used to evaluate the data and fit a simple model to $\chi(Q)$. We find that the range of a Yukawa-like segment−segment interaction potential is about 9 Å.

1. Introduction

The recent years have seen a large number of experiments aiming in the understanding of the dependence of the Flory−Huggins interaction parameter χ in binary polymer blends and diblock copolymers on temperature,[1] composition,[2,3,34,35] and pressure.[4−7] Most of the cited literature is devoted to SANS and SAXS experiments. More recently, synchrotron SAXS studies were done on the same topic.[8]

All studies mentioned above have in common that they use the well-known Flory−Huggins lattice model[9] to describe the thermodynamics of polymer blends. This approach introduces a dimensionless quantity called the χ parameter, which in the original version of the theory is a purely enthalpic quantity. To interpret the result from SANS experiments, the random phase approximation of de Gennes[10] is widely used, which contains the same χ as a wave-vector-independent parameter. The Q independence arises from the fact that χ is usually regarded as arising from a structureless, short range, monomer−monomer interaction. The spatial dependence in this approach can be modeled by $\chi \propto \delta(r)$, where $\delta(r)$ denotes the delta function. More recently, Schweizer et al. have shown in a series of ambitious papers[11] that the χ parameter reflects the direct correlations present in the system and hence should depend on the wave vector Q. This work was prompted by those papers, and we present results showing that χ is indeed a function of Q. We focus on a binary polymer blend, as it represents a conceptually simpler system than a diblock copolymer. The material chosen was a 50/50 blend of polystyrene (PS) and poly(*p*-methylstyrene) (PpMS). For this system, the temperature dependence of the Flory−Huggins parameter has been determined earlier by Londono and Wignall[12] and by Jung and Fischer.[13]

A simplified theory based on Schweizer's approach for the description of χ in terms of direct correlation functions is used to fit the data and to extract the desired quantity $\chi(Q)$. In the framework of this study, we also measured the temperature dependence of the unperturbed dimensions of PpMS, which will be published in a separate paper.[14]

The present paper is organized as follows: in the theoretical section, we present the basic features of the original Flory−Huggins lattice theory and the random phase approximation for the scattering from binary polymer blends. Then we give a brief sketch of the PRISM theory of Schweizer et al., which goes beyond mean field theory. After the description of the experiment, we present the results and give a brief conclusion.

2. Theoretical Section

2.1. Flory−Huggins Lattice Theory. The standard theory employed to the thermodynamics of polymer blends is the well- known Flory−Huggins lattice model. It mimics the repulsive forces between the segments by the requirement that one lattice site can only be occupied by a single monomer. The attractive interactions between nonbonded monomers are modeled by a mean field approach. This leads to a relatively simple form for the (excess) Helmholtz free energy ΔF of a bimodal polymer blend:[9]

$$\frac{\Delta F}{kT} = \frac{1}{N_A}\varphi_A \ln \varphi_A + \frac{1}{N_B}\varphi_B \ln \varphi_B + \chi\varphi_A\varphi_B \quad (2.1)$$

Here, $N_{A,B}$ and $\varphi_{A,B}$ denote the number of segments and the monomer concentration of species A and B, respectively. In the above notation of the free energy, the monomer concentration φ is to be understood as a segment number density. χ is the Flory−Huggins thermodynamic interaction parameter. The system has been

† Present address: Physikdepartment E13, Technische Universität München, James-Franck-Str. 1, 85747 Garching, Germany.
‡ Present address: Experiments Division/High Brilliance Beamline, European Synchrotron Radiation Facility, 6, rue Jules Horowitz, B.P. 220, F-38043 Grenoble cedex, France.

10.1021/ma010576o CCC: $22.00 © 2002 American Chemical Society
Published on Web 08/09/2002

assumed to be incompressible, reflected by the condition

$$\varphi_A + \varphi_B = 1 \tag{2.2}$$

The first two terms in eq 2.1 represent the ideal entropy of mixing of two polymer chains. Because of the connectivity of the chains (large $N_{A,B}$), these terms are rather small for long polymer chains. The last term is the enthalpy of mixing. The χ parameter is a priori a purely energetic term. Because of the small entropy of mixing, miscibility can only be achieved if χ is very small or negative. This explains why most polymer blends are immiscible.

The curve in the phase diagram, where spontaneous demixing occurs, is called the spinodal. It is defined by the condition $\partial^2\Delta F/\partial\varphi_A{}^2 = 0$. For chains of equal lengths of N segments and a 50/50 composition, this is given by

$$\chi N = 2 \tag{2.3}$$

Furthermore, χ is generally viewed as a purely segmental, hence local, quantity, which from eq 2.1 is parametrized by $\chi = A/T$, A being a system specific constant.

Experimentally, it has been shown for many systems that χ can be better represented by the empirical form

$$\chi = \frac{\Gamma_h}{T} + \Gamma_s \tag{2.4}$$

Γ_h represents the enthalpic part whereas Γ_s contains (segmental) entropic contributions.[6]

2.2. Scattering from a Binary Polymer Blend. Small-angle neutron scattering (SANS) has been proven useful to probe the thermodynamics of polymer blends over the past decade. The formula usually applied when interpreting scattering data from binary blends is the "random phase appoximation" (RPA) derived for polymeric systems originally by de Gennes.[10] de Gennes used a linear response theory to calculate the concentration fluctuations in the melt. The intermolecular interactions were treated in a mean field sense and furthermore, incompressibility of the melt was assumed. This leads to the following formula for the structure factor $S(Q)$ of a binary blend in the one-phase region:

$$S^{-1}(Q) = \frac{1}{\varphi_A N_A g_D(QR_{g_A})} + \frac{1}{\varphi_B N_B g_D(QR_{g_B})} - 2\chi \tag{2.5}$$

Here, $g_D(QR_g)$ are the respective Debye functions, given by[21]

$$g_D(Q) = \frac{2}{Q^4 R_g{}^4}(\exp(-Q^2 R_g{}^2) - 1 + Q^2 R_g{}^2) \tag{2.6}$$

R_g is the radius of gyration of the polymer chain.

Equation 2.5 has been widely used to investigate the spinodal decomposition of polymer blends (see, e.g. refs 32 and 33) and especially to determine the temperature dependence of the respective χ parameter. Again, χ is basically treated as a Q-independent parameter.

2.3. Integral Equation Theory of Polymer Blends. The original derivation of the RPA was given for electron−electron correlations in the electron gas by Pines and Nozieres.[31] In that framework, the (bare) interaction is the Coulomb interaction, and hence, it is Q-dependent. A priori, there is no reason in the case of a polymer blend this should not be the case. Schweizer et al. have developed an integral equation theory for polymer blends which allows the calculation of the Q dependence of the interaction (and hence, of χ) explicitly.

For reference, we give a brief outline of the PRISM formalism of Schweizer et al. It is beyond the scope of this paper to give a rigorous treatment of this theory; details can be found elsewhere (see below).

The reference interaction site model (RISM)[15,16] and its extension to polymers (PRISM)[11,17] is based on the idea that one can model the complex molecules as being composed of elementary units which interact by pairwise decomposable forces. In particular, in the case of polymers, one may visualize those units as the monomers or statistical segments.

The structural correlations in the melt are then described by a generalized Ornstein−Zernicke matrix integral equation, which we give for simplicity in Fourier space:

$$\mathbf{H}(Q) = \mathbf{\Omega}(Q)\mathbf{C}(Q)[\Omega(Q) + \mathbf{H}(Q)] \tag{2.7}$$

$\mathbf{H}(Q)$, $\mathbf{C}(Q)$ and $\mathbf{\Omega}(Q)$ are square matrices of rank $N_A + N_B$, where here $N_{A,B}$ denote the number of interaction sites on species A and B in the blend. More specifically, $H(r)$ comprises the elements $\rho_A\rho_B h_{\alpha_i\beta_j}(r)$, where $h(r)$, the so-called (total) *intermolecular* correlation function, is related to the *intermolecular* radial site−site distribution $g(r)$ by $h(r) = g(r) - 1$. i,j are either A or B. $\rho_{A,B}$ denotes the molecular number densities of species A and B, respectively. Hence, as an example, the notation $h_{\alpha_A\beta_B}$ means the *intermolecular* correlation of site α on species A and site β on species B.

$\mathbf{C}(r)$ is given by the elements $c_{\alpha_i\beta_j}(r)$ and denotes the *direct intermolecular* correlation function. This means that $\mathbf{C}(r)$ comprises all correlations arising from direct contacts of the segments. Finally, $\mathbf{\Omega}(r)$ is the (normalized) *intramolecular* correlation function. Hence it describes correlations along the *same* chain. The structure factor matrix for the blend is now given by the sum of the intramolecular and the intermolecular correlation function:

$$\mathbf{S}(Q) = \mathbf{\Omega}(Q) + \mathbf{H}(Q) \tag{2.8}$$

To proceed further, Schweizer et al. have made a series of assumptions which seem to hold in a polymer melt. First, explicit chain end effects are ignored.[11] This simplifies the correlation functions considerably as they are now independent of the specific site:

$$h_{\alpha_i\beta_j}(r) = h_{ij}(r) \tag{2.9a}$$

$$C_{\alpha_i b_j}(r) = C_{ij}(r) \tag{2.9b}$$

The matrix $\mathbf{\Omega}(Q)$ is diagonal, since it describes the intrachain correlations. Hence we can write

$$\Omega_{ij}(Q) = \rho_i \omega(Q)\delta_{ij} \tag{2.10}$$

Furthermore, for the purpose and within the errors of our experiment, we can set $\omega(Q)$ equal to the Debye function $g_D(QR_g)$ given by eq 2.6.

Equation 2.7 can be written in terms of only 2×2 matrices instead of square matrices of rank $(N_A + N_B)$, as the latter decompose into identical 2×2 matrices. Solving for $\mathbf{H}(Q)$, we get:

$$\mathbf{H}(Q) = (1 - \mathbf{\Omega}(Q)\mathbf{C}(Q))^{-1}\mathbf{\Omega}(Q)\mathbf{C}(Q)\mathbf{\Omega}(Q) \tag{2.11}$$

Likewise, the structure factor matrix is given by

$$\mathbf{S}(Q) = (1 - \mathbf{\Omega}(Q)\mathbf{C}(Q))^{-1}\mathbf{\Omega}(Q) \qquad (2.12)$$

The total scattering we observe in the experiment is obtained from eq 2.12 by

$$S(Q) = (b_A, b_B)\mathbf{S}(Q)\begin{pmatrix} b_A \\ b_B \end{pmatrix} \qquad (2.13)$$

b_A and b_b denote the neutron scattering length densities for species A and B, respectively.

For a two component system, Schweizer et al. have shown[11] that (2.12) together with (2.13) can be cast in a form which looks *like* the RPA but has a *Q*-dependent χ parameter in it (see also Higgins and Benoit[18] for a general formalism to convert (2.12) and (2.13) into (2.14)):

$$S^{-1}(Q) = \frac{1}{\varphi_A N_A g_D(QR_{g_A})} + \frac{1}{\varphi_B N_B g_D(QR_{g_B})} - 2\chi_{eff}(Q) \qquad (2.14)$$

where $\chi^{eff}(Q)$ is given by

$$\chi^{eff}(Q) = \frac{1}{2}(C_{AA}(Q) + C_{BB}(Q) - 2C_{AB}(Q) \qquad (2.15)$$

Hence $\chi^{eff}(Q)$ is expressed by a combination of direct correlation functions.

Equation 2.14 is the central formula in this work and will be used later in the data evaluation. As will be shown in the Experimental Section later, we will measure the left-hand side (hence the full scattering from the binary blend) and the first two terms of the right-hand side separately. The latter quantities will be accessed by measuring an isotope blend of species A and B, respectively, where essentially the unperturbed Debye functions are seen in the experiment. The desired quantity $\chi^{eff}(Q)$ is then simply obtained by subtraction.

It has to be noted that the incompressibility assumption has been imposed on the PRISM equations in a post-facto manner to arrive at (2.14). For the experimentalist it is very appealing that the familiar form of the RPA can still be used to evaluate the data. The incompressibility assumption neglects density fluctuations and cross-correlation terms between concentration and density fluctuations. This should essentially be true, as the largest part of possible density fluctuations will be subtracted out by appropriate data manipulation. Hence in eq 2.14, only the concentration fluctuations are included which contain the relevant information. We discuss the validity of the incompressibility assumption in Appendix II.

In principle, PRISM can be used to calculate $\chi^{eff}(Q)$ by solving a multidimensional system of nonlinear equations. We address the question from a different approach. In Appendix I, we show that to first order this effective function can be written as

$$\chi_{eff}(Q) = \Gamma_s\left(1 - \frac{Q^2\sigma_A{}^2}{10}\right) + \frac{\Gamma_h{}^{eff}\exp(-\sigma_{AB}/\xi)}{T(1+\xi^2Q^2)}\left(\frac{\sin(Q\sigma_{AB})}{Q\xi} + \cos(Q\sigma_{AB})\right) \qquad (2.16)$$

Here, Γ_s and $\Gamma_h{}^{eff}$ denote the entropic and enthalpic contributions as in the simple model of eq 1.4. σ_A and σ_B are proportional to the van der Waals radii of segments A and B, respectively. As shown in Appendix I, the first term in eq 2.16 has the meaning of a segmental excluded volume sphere associated with the noncombinatorial entropy of mixing. The second term consists of the Fourier transform of an effective Yukawa potential with the interaction range ξ and a lower cutoff at the mean van der Waals' radius σ_{AB}. This cutoff arises from the geometrical (hard core) extension of the monomer, which even in the SANS regime cannot be regarded as pointlike.

In our approach, we use the experimental results to get more information about the strength of noncombinatorial entropy effects and the range of the segment−segment interaction.

Note that eq 2.16 reduces to the familiar form (eq 2.4) in the limit $Q \to 0$, if we set $\Gamma_h = \Gamma_h{}^{eff}\exp(-\sigma_{AB}/\xi)(\sigma_{AB}/(\xi + 1))$.

Some brief comment should be made on why we can expect a *Q*-dependent χ parameter on physical grounds. The widely used RPA theory is a mean-field approach using essentially a hard-core repulsion for the direct correlation functions. In other words, $\chi(r) \propto \delta(r)$. All relevant physical phenomena like spinodal decomposition can be explained by using such a *Q*-independent interaction parameter, as they only need a local interaction and the connectivity of the chains. This behavior is very similar to the appearance of long range order in liquid crystals, where we have only short-range potentials as well between the molecules (the respective order parameter is the nematic director instead of the critical concentration).

In both polymers and liquid crystals, the interaction potentials depend on the distance between the interaction constituents. There is no reason for the "real" potentials to be pointlike. For this reason, the interaction parameter in polymers shows pressure dependence.[2] In the polymer blend investigated here, it is shown in this work that the screening length ξ introduced above is of the order of 10 Å and hence a *Q* dependence of χ is visible even in the SANS regime.

Table 1. Sample Characteristics

polymer	M_w (g/mol)	N	M_w/M_n
polystyrene-h_8 (h-PS)	32 000	308	1.02
polystyrene-d_8 (d-PS)	35 000	312	1.05
poly(*p*-methylstyrene-h_{10}) (h-PPMS)	63 500	538	1.04
poly(*p*-methylstyrene-d_{10}) (d-PPMS)	53 700	420	1.05

3. Experimental Section

The homopolymers were obtained from Polymer Standards Service in Mainz, Germany. Table 1 shows the characteristics of the samples. The blends were made by dissolving the components in toluene followed by precipitating the mixed polymer solutions in methanol. The precipitates were then dried in a vacuum oven at about 40 °C. The resulting glassy powder was pressed into pellets of 1 mm thickness using a hot press at 160 °C. The pellets were free of visible bubbles and were subsequently placed between two quartz glass windows. For the SANS experiment, these sample assemblies were mounted in brass heating blocks. High-temperature O-ring seals were used to prevent oxygen from entering the sample during the data acquisition process. In addition, the SANS experiments were performed under an inert gas atmosphere to further keep out the oxygen.

The actual experiment was based on eq 2.14 given in the theoretical section. The idea specific to this experiment was to measure the term on the left-hand side of eq 2.14 and the first two terms on the right-hand side in a separate experiment. To this aim, a 50/50 blend of protonated PS and deuterated PpMS was prepared (left-hand side) and two

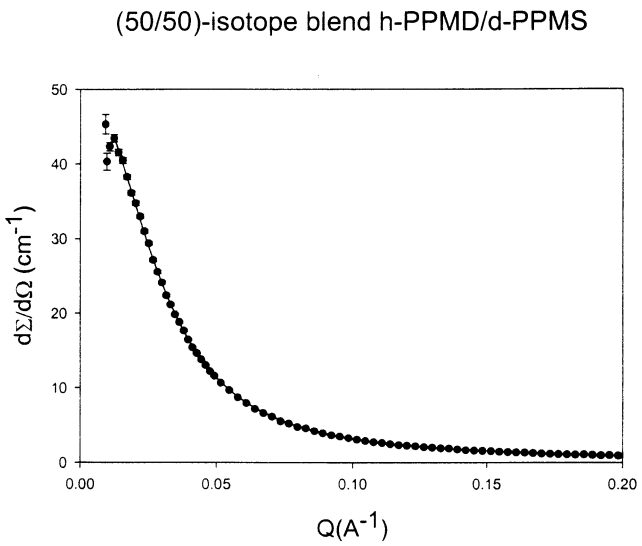

Figure 1. Data of the 50/50 isotope blend of PpMS/d-PpMS at $T = 210$ °C. The data were fitted by the Debye function. Error bars are included.

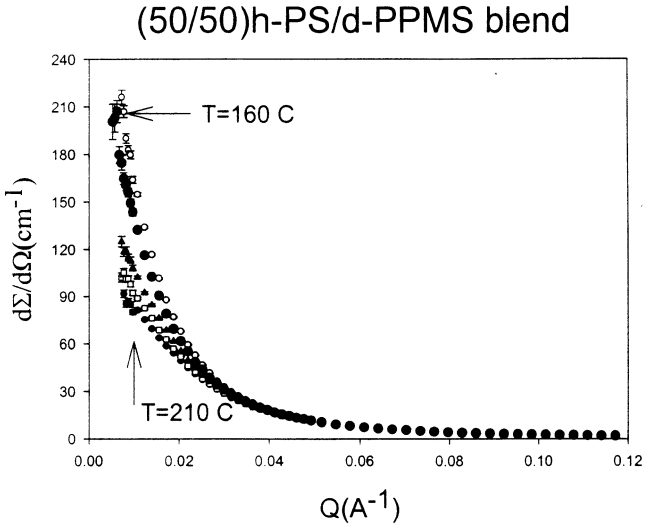

Figure 2. Data of the 50/50 h-PS/d-PpMS blend at all temperatures investigated. The critical scattering upon approaching the phase separation temperature is clearly visible.

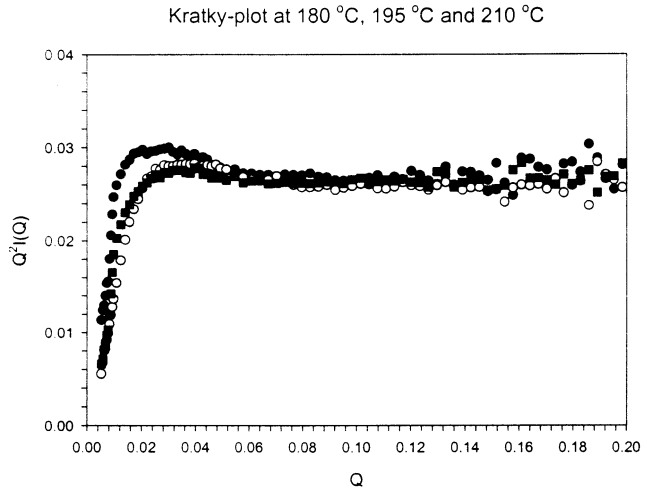

Figure 3. Kratky plots of the 50/50 h-PS/d-PpMS blend at three temperatures. The plateau shows that the background was properly subtracted.

separate 50/50 isotope blends of h-PS/d-PS and h-PpMS/d-PpMS, respectively. From the isotope blends, the unperturbed dimensions of PS and PpMS can be obtained.[27] Hence we did not rely on literature values in our experiment, but measured all required quantities. In addition to the 50/50 isotope blends, we prepared 10/90 and 20/80 mixtures of both the h-PS/d-PS and the h-PpMS/d-PpMS. By this we attempted to check if the radius of gyration changes with concentration revealing a nonnegligible χ parameter of the isotope blends. Bates et al. have reported a nonvanishing Flory−Huggins parameter for an isotope blend of high molecular weight PS.[19,23] Thus, it was necessary to examine if a residual χ occurs.

A comment on the assumption of having unperturbed dimensions of both constituents in the blend should be made. In principle, the dimensions of the individual constituents could change upon mixing. This has been found from a theoretical point of view in Monte Carlo simulations[40] and in experiments.[41] Briber et al.[41] have made a SANS study of deuterated PS in PVME. They found a slight expansion of the unperturbed dimensions of the PS chain over a reference experiment done with an isotope blend of d-PS in H−PS. However, this change in R_g was only 7%. In our case, it can be argued that PS and PpMS are much more similar in monomeric structure than PS and PVME, which have very unlike segments. Hence, if a change in R_g upon mixing occurs, it should be even smaller than the change found in Briber's work, and hence, the assumption seems to be justified.

The data were taken at the SAND instrument of IPNS at Argonne National Laboratory.[29] The pulse frequency of IPNS is 30 Hz. The sample to detector distance was fixed at 2 m; the wavelengths used ranged from 1.4 to 14 Å. This translated into a large Q range of 0.005−0.6 Å^{-1}. The detector was a 40 × 40 cm^2 area sensitive ^{3}He detector with 128 × 128 channels. Typical integration times were 2 h per sample.

The data were absolutely calibrated using a silica standard, following a routine procedure at IPNS.[30] For all temperatures, the incoherent scattering arising from the protons in the samples were measured separately. Also, transmissions have been recorded for each sample at each temperature to facilitate absolute calibration. The scattering from the empty container as well as the incoherent scattering was subtracted from the data weighted by the appropriate transmissions. Furthermore, the deuterated PS and PpMS matrices have been measured at one temperature (198 °C). The incoherent scattering from the deuterium should be negligible, but we found that the d-matrices scattered more than the calculated values, probably due to incomplete deuteration. An example for the resulting curves after doing all the corrections is shown in Figures 1 and 2. In Figure 1, the absolutely calibrated data of the 50/50 isotope blend h-PpMS/d-PPMS are displayed. Figure 2 shows the h-PS/d-PpMS-blend data at all temperatures investigated.

In Figure 3, the data are plotted in the Kratky format. This format is especially useful to check for a proper background subtraction. From the Flory-ideality assumption,[9] it is known that in the melt the chains exhibit essentially unperturbed chain statistics almost down to the monomeric level. In the intermediate Q regime, the structure factor is proportional to Q^{-2} and one should oberve a plateau plotting $Q^2 \cdot S(Q)$. We indeed find a pronounced plateau showing the validity of our background subtraction.

Temperatures were controlled within 0.1 °C in stability with an absolute precision of about 2 °C. As in general there is a gradient between the point where the temperature is measured and the interior of the quartz cells, we monitored the interior temperature by a separate sample container modified in a way that a thermocouple could be placed inside the quartz cell. Data have been collected at five different temperatures for the 50/50 blend and the isotope blend h-PpMS/d-PpMS. For the PS-isotope blend, we only recorded the lowest and the highest temperatures, because PS is a system known to have no temperature change in R_g.[20] This was confirmed by our experiments. All measurements on isotope blends were carried out at three different concentrations for reasons mentioned above.

Extraction of the Flory−Huggins parameter as a function of Q was done based on eq 2.14, which we recast here in a form directly accessible by experiment:

$$\frac{d\Sigma^{-1}}{d\Omega}(Q) = \frac{1}{\varphi_A V_A{}^w g_D(QR_{g_A})\Delta\rho^2} + \frac{1}{\varphi_B V_B{}^w g_D(QR_{g_B})\Delta\rho^2} - \frac{2\chi^{eff}(Q)}{v_0\Delta\rho^2} \quad (3.1)$$

$V_{A,B}$ are the volumes of chains A and B. v_o is a reference segmental (or monomer-) volume and conveniently expressed by $v_o = (v_A v_B)^{1/2}$. $\Delta\rho$ is the scattering length density difference given by

$$\Delta\rho = \left(\frac{\Sigma b_{A_j}}{v_A{}^{mon}} - \frac{\Sigma b_{B_j}}{v_B{}^{mon}}\right) \quad (3.2)$$

b_{A_j} and b_{B_j} denote the scattering lengths of the atoms of monomer A or B.

4. Results and Discussion

To obtain the desired quantity $\chi(Q)$ from eq 3.1, we had first to make sure that the isotope blend data can be fitted by the Debye function and hence reveal the unperturbed dimensions of PS and PpMS, respectively. This procedure implies that the isotope χ parameter is negligible. For PS, this effect has been investigated long ago by Bates et al. and by Boothroyd et al.[19,20] Bates et al.[19] showed that a small residual χ occurs for high molecular weight chains. Boothroyd et al.[20] investigated the influence of the isotope χ parameter on the unperturbed dimensions for the chain length used in his study. The largest influence on the scattering was estimated to be 6% at low Q for a 400K molecular weight chain. Our polymer samples are much lower in molecular weight; hence, no influence of a residual χ is to be expected. To make sure that this is really not the case, we have measured several concentrations as mentioned above. The data are subsequently plotted in the Zimm format.[26] The Zimm plot makes the tacit assumption that χ^{iso} is independent of the concentration. This behavior is supported by theoretical studies.[28] From the slope of the $\varphi\rightarrow 0$ extrapolation, χ^{iso} is found to be negligible. We get 2.5×10^{-4}, which is not too far off from the value of 1.72×10^{-4} by Bates et al.,[19] given all the experimental uncertainties. Figure 4 shows such a Zimm plot for the PS isotope blend at $T = 160$ °C.

The fit of the h-PpMS/d-PpMS isotope blend is included in Figure 1 to show that the Debye function fits the isotope blends very well. Given this, one could think of calculating the first two terms on the right-hand side of eq 3.1 from the parameters of the Debye-fit and subtract the calculated curves from the left-hand side. The reason for doing so would be the elimination of statistical errors caused by the isotope blend data.

This idea was checked in Figure 5, where the difference in subtracting the actual experimental data from the left-hand side of eq 3.1 vs subtracting the calculated curve (Debye function) at $T = 160$ °C is shown. At intermediate $Q > 0.04$ Å^{-1}, differences emerge. This difference can in part be attributed to the worse statistics of the direct subtraction, but in part the effect is real. As the effect we are looking for is very small, we decided to use only the data sets where the actual experimental data of the isotope blends have been subtracted.

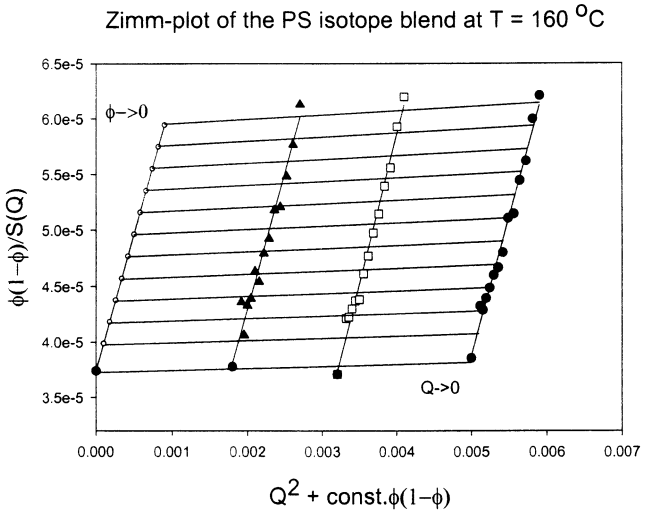

Figure 4. Zimm plot of the PS isotope blend at $T = 160$ °C. From the $Q \rightarrow 0$ extrapolation, it can be seen that the isotope χ parameter is very close to zero. The volume fraction of the deuterated species is 10% (triangles), 20% (open squares), and 50% (circles), respectively.

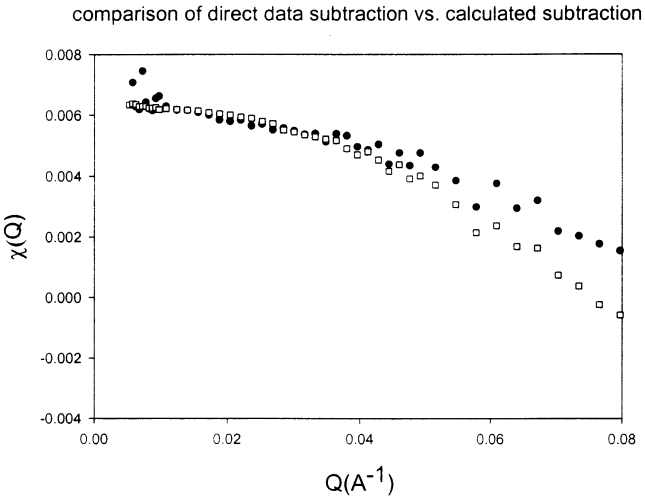

Figure 5. Comparison of a direct data subtraction (filled circles) vs the subtraction of the calculated Debye functions (open squares) from the left-hand side of eq 3.1 at $T = 160°$ C. At intermediate $Q > 0.04$ Å^{-1},differences in the two curves appear. This can on one hand be attributed to small errors in absolute calibration as well as a very small residual isotope χ parameter which would slightly distort the Debye function.

Figure 6 shows the Q dependence of the Flory−Huggins parameter for the five temperatures measured derived by the procedure described above. Clearly, χ is not a constant in Q as generally implicitly assumed in the interpretation of SANS data. On the contrary, the Q dependence seems to be rather pronounced. At low Q, the slope of the curve is smaller than at high Q, indicating a plateau. In that regime the assumption of a Q-independent Flory−Huggins parameter is reasonably well justified. Also, the decrease of χ with Q is more pronounced for the lower temperatures suggesting that the interaction length ξ is larger than at higher temperature. This effect is obscured in Figure 6 due to the large number of data points shown. Hence we replotted the data only for the lowest and the highest temperature in Figure 7 for clarity.

We attempted to fit the data by the formula (eq 2.16) given for $\chi^{eff}(Q)$ in the Theoretical Section. Leaving all

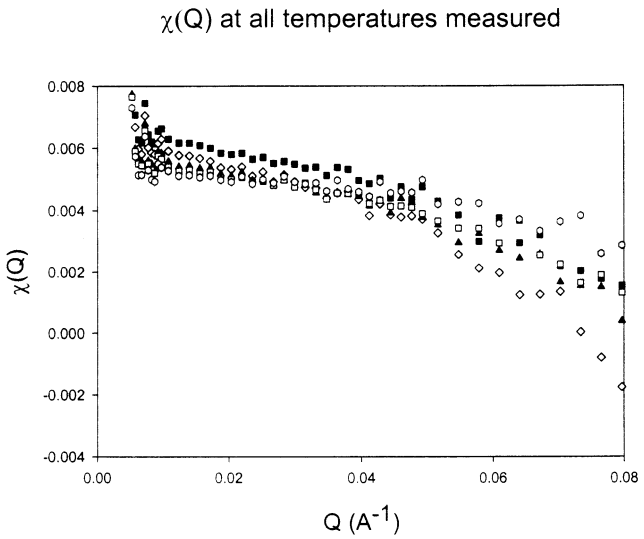

Figure 6. Q dependence of the interaction parameter χ (direct data subtraction) at all temperatures investigated. Temperatures are 160 (filled squares), 173 (open diamonds), 185 (filled triangles), 198 (open squares), and 210 °C (open hexagons), respectively. A Q dependence is clearly seen. For the lower temperatures, it is more pronounced.

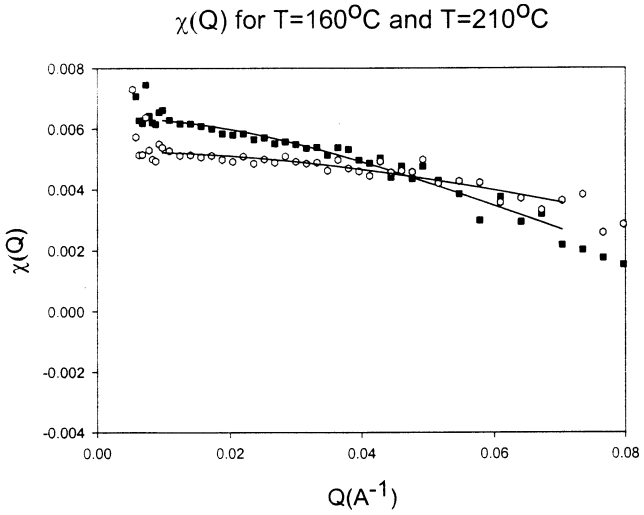

Figure 7. Plot very similar to Figure 6, but only two temperatures (160 and 210 °C) shown. The difference in curvature for the lower (filled squares) and the higher temperature (open hexagons) is clearly visible. Fits with eq 2.16 are also included.

parameters free, this fit is not stable. Hence we aimed in obtaining some of the parameters from an analysis of the $Q \rightarrow 0$ limit. We did this following the traditional approach of obtaining χ as a function of temperature. Equation 3.1 is written in the Zimm format valid at small Q:

$$\frac{d\Sigma}{d\Omega}^{-1}(Q) = \frac{1}{\Delta\rho^2 {V_A}^w \varphi} + \frac{1}{\Delta\rho^2 {V_B}^w (1-\varphi)} + \frac{Q^2}{3}\left[\frac{{R_{g_A}}^2}{\Delta\rho^2 {V_A}^w \varphi} + \frac{{R_{g_B}}^2}{\Delta\rho^2 {V_B}^w (1-\varphi)}\right] - \frac{2\chi^F}{v_o \Delta\rho^2} \quad (4.1)$$

Here we have explicitly used the term χ^F to denote that no Q dependence is assumed. In the Zimm region, this assumption is right, as can be seen from the plateau in Figure 6.

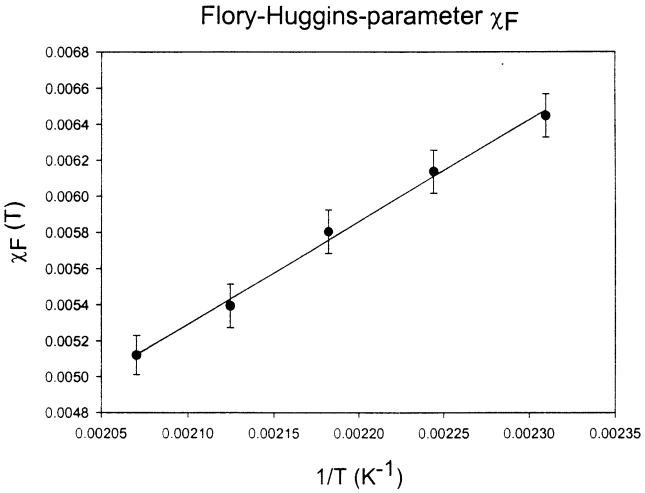

Figure 8. Low-Q (Flory−Huggins) parameter χ_F as a function of temperature.

The Flory−Huggins parameter is obtained from the intercept of a straight line fit of the inverse cross section vs Q^2. The $\chi(T,Q\rightarrow 0)$ values from the intercepts are plotted in Figure 8. They fall on a straight line when plotted vs $1/T$ as anticipated. We obtain $\Gamma_s = -(6.6 \pm 0.5) \times 10^{-3}$ and $\Gamma_h = 5.67 \pm 0.2$ K. As is shown in Appendix I, $\Gamma_s \cong -u$, a quantity reflecting the strength of noncombinatorial entropic effects. To be more precise, u can be regarded as the difference of the strength of the direct correlation function C_{AB} to the mean value of C_A and C_B. A negative Γ_s means a positive u and this in turn favors mixing of the monomers due to excess clustering of PS with PpMS monomers (see Appendix I). One could also say the system (locally on a segmental base) wins entropy by clustering different monomers.

The values of Γ_h and Γ_s are on the same order as the ones obtained by Londono et al. for a PS/PpMS system of similar molar mass and concentration.[4] The mean field spinodal temperature in our case is found to be 143 °C. In the limits of the errors, this is exactly the same temperature we would get when using the parameters for Γ_h and Γs of Londono et al. with our molar masses (which would be 142 °C). Thus, our analysis of the $Q \rightarrow 0$ limit agrees well with their results, although the parameters themselves are somewhat different.

Fixing Γ_s to the value arising from the $Q \rightarrow 0$ extrapolation, eq 2.16 could be fitted to the data. It turns out that we cannot easily separate σ and ξ, as they appear in the combination σ/ξ in the exponent. Thus, we needed to keep one parameter constant. We chose σ, as it essentially reflects the van der Waals radius of the segments and experimental values are available. We used a publication by Bondi[24] to get an estimate of the van der Waals volumes of the PS and the PpMS monomer units, respectively. The Bondi paper uses a group contribution method to estimate van der Waals volumes of larger chemical units. We estimated the van der Waals radii by assuming a spherical shape. We obtained 3.0 Å for σ^{PS} and 3.2 Å for σ^{PpMS}. We are aware that there a more recent studies on van der Waals radii using more sophisticated methods than the ones Bondi was using.[25] However, for our purpose, a rough estimate of σ is sufficient.

In the fits, we need σ_A as well as σ_{AB}. We simply used the mean value of PS and PpMS, 3.1 Å, for the latter. Fixing B and σ, we obtain stable fits for ξ and Γ^{eff} using eq 2.16. The fits are displayed for the 160 °C data and

Table 2. Results of the Fits with Model (Eq 2.16)

T (°C)	ξ (Å)	Γ_h^{eff} (K)
160	8.6 ± 0.3	5.92 ± 0.02
173	10.4 ± 0.3	5.87 ± 0.03
185	8.5 ± 0.2	5.92 ± 0.02
198	7.7 ± 0.4	6.20 ± 0.02
210	5.2 ± 0.3	6.51 ± 0.02

Table 3. Results of Fit with Thread Limit Model (Eq 4.3)

T (°C)	ξ (Å)	Γ_h (K)
160	8.7 ± 0.3	5.61 ± 0.03
173	10.6 ± 0.3	5.66 ± 0.03
185	8.7 ± 0.2	5.60 ± 0.02
198	8.0 ± 0.2	5.67 ± 0.03
210	5.5 ± 0.3	5.72 ± 0.03

the 210 °C data of $\chi(Q)$ in Figure 7. The results for all temperatures are shown in Table 2.

We only obtained reasonable fits if we restrain Q to be smaller than about 0.065 A^{-1}. This shows that the underlying assumption of formula 2.16 (or A11), namely that $C(r)$ can be expressed solely by the first term in the expansion (eq A2) (see Appendix I), is valid only for low Q. In other words, at low Q, which corresponds to large distances, it is sufficient to approximate the direct correlation function by a hard sphere only. At larger Q, however, this seems to break down, and a more sophisticated model for $C(r)$ is needed.

In view of the above, we were interested what values for ξ would emerge from the thread−polymer idealization of Schweizer and Curro.[22] It is a further simplification of the hard core potential and basically states that the hard core diameters $\sigma \rightarrow 0$ in a manner leaving the (monomer) density finite. Then $\chi(r)$ can be written as

$$\chi(r) = \Gamma_s \delta(r) - \frac{v_{AB}(r)}{T} \tag{4.2}$$

where $v_{AB}(r)$ is the Yukawa potential (eq A3). The first term is again the hard core repulsion, the second term the weakly attractive potential. Clearly, this equation cannot describe the details of the interaction on a very local scale by construction, but it should be valid at low Q. Fourier transforming eq 4.2, we simply obtain

$$\chi(Q) = \Gamma_s + \frac{\Gamma_h}{T(1 + Q^2\xi^2)} \tag{4.3}$$

Γ_h and Γ_s are the exact counterparts to eq 2.4 in the theoretical section (which evidently is the $Q \rightarrow 0$ limit). Again, we left Γ_s constant and fitted Γ_h and ξ to the data. The results are shown in Table 3. They do not differ much from the results of the explicit hard core model. This demonstrates that the crucial assumption of thread-like polymer chains is valid in the low Q limit. $2\pi/Q$ gives an estimate for the corresponding real space distance. From this, we observe that on length scales of about 100 Å the assumption is valid.

One can clearly see that the interaction range ξ is slightly temperature dependent. At high temperatures, far away from the phase separation temperature, ξ is smaller than closer to the phase transition, where it seems to level off to a constant value of about 8.5 Å.

We also attempted to obtain ξ from a fit of the Zimm region only. Recalling eq 4.1 and using $\chi(Q) = \Gamma_s + \Gamma_h/T(1 - Q^2\xi^2)$ (from eq 4.3 for small Q), we can estimate ξ from the slope α of the Zimm fit:

$$\alpha = \frac{1}{3}\left(\frac{R_{g_A}^2}{\varphi N_A} + \frac{R_{g_B}^2}{(1-\varphi)N_B}\right) + \frac{2\Gamma_h}{T}\xi^2 \tag{4.4}$$

The Zimm analysis has a clear advantage over the model (eq 2.16) in that the fit is just a straight line and hence conceptually much simpler.

Table 4 shows the result. The error in ξ is estimated to be about 0.8 Å for all temperatures. The results follow the same trend; with decreasing temperature (closer to the phase transition) the interaction range is increasing. Thus, by using three different evaluation methods, one obtains very similar results for the main quantity of interest, the range ξ of the segment−segment interaction potential. To examine whether this temperature dependence is specific to the system chosen or of more general character, more experiments on different isotope blends should be performed.

To our knowledge, two more groups have examined the q dependence of the χ parameter. Brereton et al.[42] have investigated three different binary mixtures. One of the systems corresponds to the system used in the present work. They give a simple form of $\chi(Q) = \chi°(1 - KQ^2)$ which is an ad hoc assumption. This form is similar to the low-Q limit of eq 4.3 if we identify $\chi°$ with Γ_h/T and neglect Γ_s. The main purpose of Brereton et al. was to investigate the very anomalous behavior of the mixture polytetramethy carbonate/polystyrene. All the analysis is based on the simple model for $\chi(Q)$ given above and is restricted to very small Q (Zimm region). They extract K from the intercept of a plot of a quantity $S_o(T)(l^2 + 2K\chi_S) - K$ vs $S_o(T)$ for several temperatures. As the effect found in polytetramethy carbonate/polystyrene is orders of magnitude larger than in PS/PpMS, the authors only give the comment that, in the latter case, the data are consistent with K being about zero without doing a thorough analysis of this system.

Balsara et al.[34] evaluated data from several polyolefine blends using a method similar to ours to evaluate $\chi(Q)$. They define an excess function $E(Q)$, which corresponds to our $\chi(Q)$. A small Q dependence of χ is found, but the data show an upward curvature. We found χ to be a decreasing function of Q. Hence, the results disagree with our findings. The origin of the discrepancy cannot be explained at the present state, but we believe that this may be because a different system was used in ref 34. In addition, the authors did not do the experiments with the main purpose of evaluating $\chi(Q)$ but in order to obtain the concentration dependence of χ. The present work was especially designed to evaluate the Q dependence. Further measurements should be done in order to solve the discrepancy.

5. Conclusion

We have shown that SANS can be used to address the question of the Q dependence of the Flory−Huggins interaction parameter χ in a binary polymer blend. Contrary to the assumption that χ can be viewed as a merely local quantity with a spatial dependence proportional to $\delta(r)$, our data show a striking Q dependence even in the SANS regime except for low Q. Moving to higher Q values, χ is clearly not a constant and falls off as a function of Q. We attempted to find a model to describe the observed behavior and which at the same time preserves the familiar form $\chi = \Gamma_h/T + \Gamma_s$ in the limit of $Q \rightarrow 0$. This model has the interaction range ξ of a Yukawa like segment−segment potential and the

Table 4. Results of Zimm Analysis (Eq 3.1)

T (°C)	ξ (Å)
160	8.8 ± 0.8
173	9.1 ± 0.8
185	8.2 ± 0.8
198	7.7 ± 0.8
210	6.4 ± 0.8

hard core (essentially the van der Waals') radii of the segments as additional parameters. The interaction range is found to depend on temperature, it increases from about 6 to about 9 Å when lowering the temperature from 210 to 160 °C. These values did not change significantly for the three models used in the analysis (see sections 3 and 4).

The parameter Γ_s has been given an explicit meaning. It describes noncombinatorial (segmental) entropy effects. Hence the underlying assumption of the original Flory−Huggins theory that a splitting of entropic and enthalpic effects can be made (see eq 2.1) is too simple. Instead, the enthalpic term of the Helmholtz free energy proportional to χ contains part of the entropy as well. This notion is not entirely new, but an explicit explanation for Γ_s has been given in the present work.

Acknowledgment. We thank Lew Fetters for the GPC determination of the molecular weights of our polymer samples and Wim Pyckhout-Hintzen and Walter Schirmacher for helpful comments and discussions. We would also like to thank D. G. Wozniak (IPNS) for his technical help. This work was supported by the Department of Energy (Grant DE-FG02-97ER62443). This work also benefited from the use of the Intense Pulsed Neutron Source, which is funded by the U.S. Department of Energy, Office of Basic Energy Sciences, under Contract W-31-109-ENG-38 to the University of Chicago.

Appendix I

In Appendix I, we derive formula 2.16 from considerations on the general form of the interaction parameter χ. Expressed by the direct intermolecular correlation functions, $\chi^{\text{eff}}(Q)$ is given by

$$\chi^{\text{eff}}(Q) = \frac{1}{2}(C_{\text{AA}}(Q) + C_{\text{BB}}(Q) - 2C_{\text{AB}}(Q) \quad \text{(A1)}$$

We see that the Q-independent Flory−Huggins parameter has been replaced by a combination of *direct correlation functions*. We use the form for the $C(Q)$ (or $C(r)$ in the first place) suggested by PRISM to proceed in the calculation of χ. Intuitively, we may argue that the $C(Q)$ are basically given by effective pair potentials in a dense fluid and hence we can say that $\chi(Q)$ basically probes those pair interactions.

As it turns out, the calculation of the direct correlation functions is not possible without appropriate closures. Schweizer et al. have used several different approaches over the past decade for those closures. We wanted to follow a route where we can get an approximate analytic expression for $\chi(Q)$ which we can compare to our data. Hence, we employ one of the simplest closures available for $C(r)$:[11]

$$C_{\text{ij}}(r) = \begin{cases} \sum_{k=1}^{4} a^{\text{kij}} \left(\frac{r - \sigma_{\text{ij}}}{\sigma_{\text{ij}}}\right)^{k-1}, & r < \sigma_{\text{ij}} \\ \frac{v_{\text{ij}}}{kT}, r > \sigma_{\text{ij}} \end{cases} \quad \text{(A2)}$$

This is the mean spherical approximation closure (MSA). The idea is basically that inside the hard core given by the σ_{ij} we can approximate the direct correlation functions by polynomials in $(r - \sigma)/\sigma$ and outside by a weak attractive potential $v_{\text{ij}}(r)$ which is realistically of the Lennard-Jones type. σ_{ij} can be identified with the van der Waals' radii of the respective segments. The a_k^{ij} are coefficients describing the strength of the respective term in the expansion. In principle, one could solve the PRISM equations and obtain the coefficients a_k^{ij} using the closure (eq A2), but a direct solution using realistic potentials and parameters σ for our polymers is beyond the scope of this work. Thus, we seek for a simplified expression of eq A2, which contains a few experimentally accessible parameters we can fit to the data.

The first step lies in a Fourier transform of $C(r)$. This can be done analytically if we assume a Yukawa potential[11,22] for the interaction potential between species A and B and set $v_{\text{ii}}(r)$, the potential between like segments, equal to zero. At high densities in the melt, this assignment mimics the mutual interactions quite accurately.

Hence we have

$$v_{\text{AB}}(r) = \frac{\epsilon \exp(-r/\xi)}{r/\xi}$$
$$v_{\text{AA}} = v_{\text{BB}} = 0 \quad \text{(A3)}$$

ξ is the screening length of the potential and is effectively a measure for the interaction range. ϵ is a parameter denoting the strength of the interaction. The above assignment of the interactions can be explained by recalling that for species A and B, there are repulsive and attractive interactions present with regard to their own species and with regard to the other species. Setting v_{AA} and v_{BB} equal to zero and describing v_{AB} by a (weak) Yukawa potential reflects the fact that the A−A and B−B interactions are different from the A−B interactions. In general, the latter are slightly more repulsive than the former (but the difference is small). Hence ϵ is small but positive in most cases. One could also visualize v_{AB} as an excess potential with regard to v_{AA} and v_{BB}.

We would like to note that in binary alloys, the effective ordering potential is of a similar form as our effective χ parameter. In binary liquids, the concentration fluctuations also give rise to an effective pair interaction as has been shown by Ruppersberg and Schirmacher.[36,37] They make use of the MSA closure for the direct correlation functions as well to describe neutron diffraction data from liquid Li_4Pb and Li_7Ag_3.

The Fourier transform of eq A2 is a rather lengthy expression. $C_{\text{AA}}(Q)$ and $C_{\text{BB}}(Q)$ are both given by

$$\frac{C(Q)}{4\pi} = a_1\left(\frac{\sin(Q\sigma) - Q\sigma\cos(Q\sigma)}{Q^3}\right) + a_2\left(\frac{2\cos(Q\sigma) + Q\sigma\sin(Q\sigma)}{Q^4\sigma} - \frac{2}{Q^4\sigma}\right) + a_3\left(\frac{2Q\sigma\cos(Q\sigma) - 6\sin(Q\sigma)}{Q^5\sigma^2} + \frac{4}{Q^4\sigma}\right) + a_4\left(\frac{-24\cos(Q\sigma) - 6Q\sigma\sin(Q\sigma)}{Q^6\sigma^3} - \frac{6Q^2\sigma^2 - 24}{Q^6\sigma^3}\right) \quad \text{(A4)}$$

where we have left out the subscripts A and B for clarity. $C_{AB}(Q)$ is given by an expression of exactly the same form, but an additional term due to the Yukawa potential appears. It is not just the Fourier transformation of the Yukawa potential we have to calculate, which would just be a Lorentzian, but the integral has σ_{AB} as a lower limit:

$$v_{AB}(Q) = \frac{4\pi}{Q}\int_0^\infty r\sin(Q\sigma_{AB})\epsilon\frac{\exp(-r/\xi)}{r/\xi}\,dr = \frac{4\pi\xi^3\epsilon\exp(-\sigma_{AB}/\xi)}{1+\xi^2Q^2}\times\left(\frac{\sin(Q\sigma_{AB})}{Q\xi} + \cos(Q\sigma_{AB})\right) \quad \text{(A5)}$$

A note has to be made on the dimensions $C(Q)$. As the theory is usually written down in terms of dimensionless quantities, $\chi(Q)$ and hence $C(Q)$ should be dimensionless as well. Equations A4 and A5, on the other hand, yield the dimensions of a volume. To make $C(Q)$ dimensionless, one has to divide by a volume. We choose the monomer volume as a natural volume here for reasons which will become apparent later. For now, we just keep in mind that such a division has to be made in order to make $C(Q)$ dimensionless.

It becomes immediately evident that the combination of $C_{AA}(Q)$, $C_{BB}(Q)$, and $C_{AB}(Q)$ has too many parameters to be fitted to the experiment. There are 12 coefficients a^{ij}, three parameters σ_{ij}, and the interaction length ξ. But keeping in mind that we want to compare to a SANS experiment and hence that the Q values are in a range where $Q\sigma \ll 1$ holds for the most Q, we can expand the $C_{ij}(Q)$ in a Taylor series. This yields the following expression for C_{AA} and C_{BB}:

$$\frac{C(Q)}{4\pi} = \left(\frac{a_1}{3} - \frac{a_2}{12} + \frac{a_3}{30} - \frac{a_4}{60}\right)\sigma^3 + \left(\frac{-a_1}{30} + \frac{a_2}{180} - \frac{a_3}{630} + \frac{a_4}{1680}\right)\sigma^5Q^2 \quad \text{(A6)}$$

For C_{AB}, we have to add the term resulting from the potential (eq A4):

$$\frac{4\pi\xi^3\epsilon\exp(-\sigma_{AB}/\xi)}{T}\left\{\left(\frac{\sigma_{AB}}{\xi}+1\right) + \left(\frac{-\sigma_{AB}^3}{6\xi} - \frac{\sigma_{AB}^2}{2} - \left(\frac{\sigma_{AB}}{\xi}+1\right)\xi^2\right)Q^2\right\} \quad \text{(A7)}$$

However, it turns out that the fit is more stable when using the full expression (eq A5) for the potential instead of the Taylor series (eq A7). Thus, we retain (A5) in the expression for $\chi_{eff}(Q)$.

A close inspection of eq A6 shows that it will not be possible to distinguish between the coefficients a_i by the experiment in the SANS regime. One could combine all four coefficients into a single one and fit an expression $b - cQ^2$ to the data. The most general expression encompassing the form of eqs A5 and A6 is given by

$$\chi_{eff}(Q) = \beta_1 - \beta_2Q^2 + \frac{\Gamma_h^{eff}\exp(-\sigma_{AB}/\xi)}{T(1+\xi^2Q^2)}\left(\frac{\sin(Q\sigma_{AB})}{Q\xi} + \cos(Q\sigma_{AB})\right) \quad \text{(A8)}$$

Γ_h^{eff}, β_1, and β_2 are parameters including all coefficients appearing in (A5−A7). We note that the limit $Q \to 0$ coincides with the familiar form of eq 2.4 if we set Γ_h in eq 2.4 $= \Gamma_h^{eff}\exp(-\sigma/\xi)(\sigma/(\xi+1))$. From this relation, it becomes evident again that Γ_h in (2.4) is very closely related to the enthalpic part of the interaction.

β_1 and β_2 contain a lot of hidden parameters (in particular the a_i) and their actual meaning is not obvious. If we retain only the first term in each of the brackets in the expansion of $C(Q)$ (eq A6), we obtain a more illuminating expression for $\chi_{eff}(Q)$:

$$\chi^{eff}(Q) = \frac{1}{2}\left[a_A\frac{4\pi}{3}\sigma_A^3\left(1 - \frac{Q^2\sigma_A^2}{10}\right) + a_B\frac{4\pi}{3}\sigma_B^3\left(1 - \frac{Q^2\sigma_B^2}{10}\right) - a_{AB}\frac{4\pi}{3}\sigma_{AB}^3\left(1 - \frac{Q^2\sigma_{AB}^2}{10}\right)\right] + \frac{\Gamma_h^{eff}\exp(-\sigma_{AB}/\xi)}{T(1+\xi^2Q^2)}\left(\frac{\sin(Q\sigma_{AB})}{Q\xi} + \cos(Q\sigma_{AB})\right) \quad \text{(A9)}$$

Here, we have omitted the subscript 1 on the coefficients a_I and added all terms C_{ij} as demanded by eq A1. Retaining only the first terms amounts to approximating the direct correlation functions by spheres only.

What does this expression mean? In real solutions, it is known that upon mixing there is usually an enthalpy change. The analogue for our case of the bimodal melt is the last term in (2.1). But in addition, there may also be a contribution to the entropy change apart from the ideal mixing term given in eq 2.1. This term arises from the way that the segments of one type might cluster together instead of mixing with the others. The first three terms of eq A9 reflect this excess entropy, which we might also call non combinatorial entropy. If A = B (both species are the same), these terms would vanish, of course. If A ≠ B, there is an excess (segmental) entropy basically proportional to the difference in the (segmental) excluded volume spheres of species A, B and the "mixed" sphere built by the average excluded volume of A and B.

Equation A9 can be expanded further, if we make the following assumptions:

$$\sigma_B = \sigma_A + \delta \qquad a_B = a_A + \eta \qquad a_{AB} = (a_A + a_B)/2 + u \qquad \sigma_{AB} = (\sigma_A + \sigma_B)/2 \quad \text{(A10)}$$

where δ, η, and u are small. The last two equations in (A10) need to be explained a little further. The first one assumes that the strength of the correlation function C_{AB} is given by the average value of C_A and C_B plus a

small constant which accounts for the fact that a_{AB} usually is not just additive. It is an assumption, though, that u is small. The last equation states that the (effective) mean van der Waals' radius is just the average of σ_A and σ_B. This is an assumption, too, and one could have added a small constant as well. But this constant is included in u, because a_{AB} is multiplied with powers of σ_{AB}, and to first order, it does not matter whether we add another small constant to σ_{AB}.

Inserting (A10) into (A9) and neglecting all higher order terms of $O(2)$ in δ, η, and u, we obtain

$$\chi_{eff}(Q) = \Gamma_s\left(1 - \frac{Q^2{\sigma_A}^2}{10}\right) + \frac{{\Gamma_h}^{eff}\exp(-\sigma_{AB}/\xi)}{T(1+\xi^2Q^2)} \times \left(\frac{\sin(Q\sigma_{AB})}{Q\xi} + \cos(Q\sigma_{AB})\right) \quad \text{(A11)}$$

where $\Gamma_s = (-4\pi/3)u{\sigma_A}^3$. Γ_s still has the dimension of a volume while it should be dimensionless. We now have to divide by the monomer volume, as mentioned above. This seems to be the natural choice to render the Fourier transform dimensionless. We can (somewhat arbitrarily) set A equal to PS and divide by the monomer volume of PS. Setting $\sigma_A = 3.0$ Å, we see that the result of the division is on the order of 1. Hence we obtain the interesting conclusion that $\Gamma_s \cong -u$. This holds also for the $Q \rightarrow 0$ limit. Hence, we have found an interpretation for the parameter Γ_s, which usually is used as a mere fit parameter. Γ_s is the difference of the interaction strength of the direct correlation function C_{AB} to the average interaction strengths of C_A and C_B. This directly reflects the non combinatorial entropy. If $u > 0$, Γ_s is negative and there will be a tendency of monomers of the opposite species to cluster together which favors mixing. Likewise, if $u < 0$, Γ_s is positive, and the monomers of the same species will cluster. Again, it has to be stressed that we talk about the noncombinatorial entropy effects and not about the enthalpy.

A more thorough investigation of noncombinatorial entropy effects of the Flory χ parameter was done by Freed et al.[38] in the framework of the lattice cluster expansion theory[39] and should hence be mentioned here. This theory is much more involved than the present "semitheoretical" approach. The entropic part of χ is calculated for different branching structures. In the majority of the cases, this part is negative favoring mixing of the two components. This coincides with our results for Γ_s, which appears to be negative as well.

Appendix II

In Appendix II, we show that for the system investigated in the present work, the incompressibility assumption is valid within the approximations made.

Schweizer realized that in order to calculate thermodynamic properties in dense systems, the incompressibility route could lead to wrong results.[43] He extended therefore the theory to take this problem into account by formulating an effective incompressibility condition which can be written as

$$-\rho_M\omega_M(Q)C_{MM'}(Q) \gg 1 \quad \text{(B1)}$$

where ρ denotes the density, ω_M the form-factor of species M and $C_{MM'}$ the direct correlation function of M with M′.

This relation is generally true in a dense liquid, at least for small Q. Using this condition, Schweizer derives a more complicated expression for the effective interaction parameter $\chi(Q)$:

$$\chi(Q) = \frac{\rho}{2\sqrt{C_AC_B}}(C_AC_B - {C^2}_{AB}) + \frac{1-\sqrt{C_B/C_A}}{2\Phi_A\omega_A} + \frac{1-\sqrt{C_A/C_B}}{2\Phi_B\omega_B} \quad \text{(B2)}$$

where $C_{AA}(Q)$ and $C_{BB}(Q)$ have been abbreviated by C_A and C_B, respectively.

Using this expression for χ, the scattering function $S(Q)$ can again be written in the familiar RPA form:[43]

$$S^{-1}(Q) = \frac{1}{\Phi_A\omega_A(Q)} + \frac{1}{\Phi_B\omega_B(Q)} - 2\chi(Q) \quad \text{(B3a)}$$

Now it is to be shown that for our case of a PS/PPMS blend, this χ parameter is to a very good approximation given by the χ^{eff} used in the data evaluation:

$$\chi^{eff} = \frac{\rho}{2}(C_A + C_B - 2C_{AB}) \quad \text{(B3b)}$$

We first show that C_B can be very well approximated by

$$C_B = C_A + \gamma \quad \text{(B4)}$$

where γ is independent of Q and $\ll C_A$.

To show this, we recall the form for the direct correlation functions given in the paper (eq A9):

$$C_A = a_A\frac{4\pi}{3}\left(1 - \frac{Q^2{\sigma^2}_A}{10}\right)$$
$$C_B = a_B\frac{4\pi}{3}\left(1 - \frac{Q^2{\sigma^2}_B}{10}\right) \quad \text{(B5)}$$

We then obtain γ by simply setting

$$\gamma = \frac{4\pi}{3}(a_B{\sigma^3}_B - a_A{\sigma^3}_A) \quad \text{(B6)}$$

Plotting now C_B as given by (B4) vs C_B as given by (B5), we find that the maximum difference at $Q = 0.1$ Å^{-1} is only 4×10^{-3}. This value can clearly not be distinguished by experiment. Figure 9 proves the validity of this statement.

Next we demonstrate that the last two terms in eq B2 can be neglected. We start with

$$\sqrt{\frac{C_A}{C_B}} \approx 1 - \frac{\gamma}{2C_A}$$

and likewise

$$\sqrt{\frac{C_B}{C_A}} \approx 1 + \frac{\gamma}{2C_A}$$

Inserting this into (B2), the last two terms yield together with $\Phi_B = (1 - \Phi_A)$:

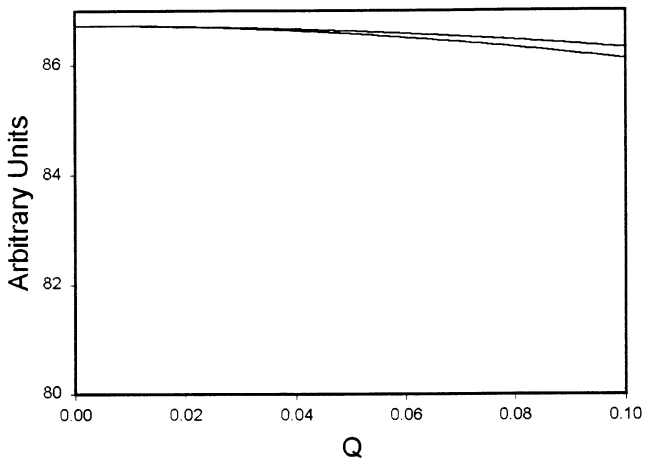

Figure 9. Comparison of the direct correlation function $C_b(Q)$ as calculated from eq B4 (upper curve) in Appendix II vs that from eq B5 (lower curve). The difference between the two curves is very small.

$$\frac{\gamma}{4\Phi C_A}\left[\frac{1}{\omega_A} - \frac{1}{\omega_B}\right] \tag{B7}$$

As the two form factors are similar and the prefactor of (B7) $\ll 1$, the last two terms in (B2) can be neglected. Then we obtain

$$\chi(Q) = \frac{\rho}{2\sqrt{C_A C_B}}(C_A C_B - C^2{}_{AB}) \tag{B8}$$

$C_{AB}(Q)$ was also derived in Appendix I to be given by

$$C_{AB} = a_{AB}\sigma^3{}_{AB}\left(1 - \frac{Q^2\sigma^2{}_{AB}}{10}\right) - \beta v_{AB} \tag{B9}$$

$v_{AB}(Q)$ is the weakly attractive interaction potential between species A and B and β is the inverse temperature. We also recall the approximations made in eq (A10) in Appendix I. To show that the resulting expression for $\chi(Q)$ from (B8) will be similar to eq A11, we insert these approximations into C_A, C_B and C_{AB}. Again we neglect all higher order terms in δ, η, and u and, additionally, in βv_{AB}. A lengthy but conceptually simple calculation yields

$$\chi(Q) = \left[-\frac{4\pi}{3}\sigma_A{}^3 u\left(1 - \frac{Q^2\sigma_A{}^2}{10}\right) + \beta v_{AB}(Q)\right]\left(1 - \frac{\gamma}{2C_A}\right) \tag{B10}$$

The precise form of the potential is given by eq A9 or eq A11. Substituting Γ_s for the prefactor $-4\pi/3\sigma_A{}^3 u$, we obtain the same expression as given by eq A11 except for an overall scaling factor of $(1 - \gamma/2C_A)$. This means that within the approximations made, the more general interaction parameter given in ref 3 and by eq 1 and the simpler RPA-like form used in the paper are (almost) identical.

Hence we have shown that in the case of a 50/50 blend of PS and PpMS, the incompressibility assumption leads to experimentally indistinguishable results from the more elaborate effective incompressibility assumption.

The ultimate cause for the validity of the IRPA is that in SANS, we measure at low Q. In this region, the main Q dependence comes from the interaction potential and not form the direct correlation functions and an approximation as, e.g., made in eq B4 is valid.

References and Notes

(1) Rudolf, B. *Macromol. Chem. Phys.* **1995**, *196*, 4057.
(2) Rabeony, M.; Lohse, D. J.; Garner, R. T.; Han, S. J.; Graessley, W. W.; Migler, K. B. *Macromolecules* **1998**, *31*, 6511.
(3) Koch, T.; Strobl, G. R. *J. Polym. Sci., Part B: Polym. Phys.* **1990**, *28*, 343.
(4) Londono, J. D.; Narten, A. H.; Wignall, G. D.; Honell, K. G.; Hsieh, E. T.; Johnson, T. W.; Bates, F. S. *Macromolecules* **1994**, *27*, 2864.
(5) Janssen, S.; Schwahn, D.; Mortensen, K.; Springer, T. *J. Phys. (Paris) IV* **1993**, *17*, 3.
(6) Janssen, S.; Schwahn, D.; Mortensen, K.; Springer, T. *Macromolecules* **1993**, *26*, 5587.
(7) Frielinghaus, H.; Schwahn, D.; Mortensen, K.; Almdal, K.; Springer, T. *Macromolecules* **1996**, *29*, 3263.
(8) Hajduk, D. A.; Urayama, P.; Gruner, S. M.; Erramili, S. (others), *Macromolecules* **1995**, *28*, 7148.
(9) Flory, P. J. *Principles of Polymer Chemistry*; Cornell University: Ithaca, NY, 1953.
(10) de Gennes, P. G. *Scaling Concepts in Polymer Physics*; Cornell University: Ithaca, NY, 1979.
(11) A very good review of PRISM in bimodal melts is given in: Schweizer, K. S.; Curro, J. G. *J. Chem. Phys.* **1989**, *91*, 5059. For diblock copolymers, see: David, E. F.; Schweizer, K. S. *J. Chem. Soc., Faraday Trans.* **1995**, *91*, 2411.
(12) Londono, J. D.; Wignall, G. D. *Macromolecules* **1997**, *30*, 3821.
(13) Jung, W. G.; Fischer, E. W. *Makromol. Chem, Macromol. Symp.* **1988**, *16*, 281.
(14) Urban, V.; Thiyagarajan, P.; Zirkel, A.; Gruner, S. M. To be published.
(15) Chandler, D.; Andersen, H. C. *J. Chem. Phys.* **1972**, *57*, 1930.
(16) Lowden, L. J.; Chandler, D. *J. Chem. Phys.* **1973**, *59*, 6587.
(17) Curro, J. G.; Schweizer, K. S. *J. Chem. Phys.* **1987**, *87*, 1842.
(18) Higgins, J. S.; Benoit, H. *Polymers and Neutron Scattering*; Clarendon Press: Oxford, England, 1994.
(19) Bates, F. S.; Wignall, G. D.; Koehler, *Macromolecules* **1986**, *19*, 932.
(20) Boothroyd, A. T.; Rennie, A. R.; Wignall, G. D. *J. Chem. Phys.* **1993**, *99*, 9135.
(21) Debye, P. *J. Phys. Colloid Chem.* **1947**, *51*, 18.
(22) Schweizer, K. S.; Curro, J. G. *Chem. Phys.* **1990**, *149*, 105.
(23) Bates, F. S.; Wignall, G. D. *Phys. Rev. Lett.* **1986**, *57*, 1429.
(24) Bondi, A. *J. Phys. Chem.* **1964**, *68*, 441.
(25) Badenhoop, J. K.; Weinhold, F. *J. Chem. Phys.* **1997**, *107*, 5422.
(26) Zimm, B. H. *J. Chem. Phys.* **1948**, *16*, 1093.
(27) Krishnamoorti, R.; Graessley, W. W.; Zirkel, A.; Richter, D.; Lohse, D. J.; Fetters, L. J. To be published.
(28) Melenkevitz, J.; Crist, B.; Kumar, S. K. *Macromolecules* **2000**, *33*, 6869.
(29) Thiyagarajan, P.; Urban, V.; Littrell, K.; Ku, C.; Wozniak, D. G.; Belch, H.; Vitt, R.; Toeller, J.; Leach, D.; Haumann, J. R.; Ostrowski, G. E.; Donley, L. I.; Hammonds, J.; Carpenter, J. M.; Crawford, R. K. The Performance of the Small-Angle Diffractometer, SAND at IPNS. *ICANS XIV−The Fourteenth Meeting of the International Collaboration on Advanced Neutron Sources*; June 14−19, 1998, Starved Rock Lodge, Utica, IL, 1998; Vol. 2, pp 864−878.
(30) Thiyagarajan, P.; et al. *J. Appl. Crystallogr.* **1997**, *30*, 280.
(31) Pines, D.; Nozieres, P. *The Theory of Quantum Liquids*; Benjamin: New York, 1966; Vol. 1.
(32) Schwahn, D.; Mortensen, K.; Springer, T.; Yee-Madeira, H.; Thomas, R. *J. Chem. Phys.* **1987**, *87*, no. 10, 6078.
(33) Schwahn, D.; Hahn, K.; Streib, J.; Springer, T. *J. Chem. Phys.* **1990**, *93*, 8383.
(34) Balsara, N. P.; Fetters, L. J.; Hadjichristidis, N.; Lohse, D. J.; Han, C. C.; Graessley, W. W.; Krishnamoorti, R. *Macromolecules* **1992**, *25*, 6137.
(35) Krishnamoorti, R.; Graessley, W. W.; Balsara, N. P.; Lohse, D. J. *J. Chem. Phys.* **1994**, *100*, 3894.
(36) Copestake, A. P.; Evans, R.; Ruppersberg, H.; Schirmacher, W. *J. Phys. F: Met. Phys.* **1983**, *13*, 1993.
(37) Ruppersberg, H.; Schirmacher, W. *J. Phys. F: Met. Phys.* **1984**, *14*, 2787.
(38) Freed, K. F.; Adriani, I. P. *J. Chem. Phys.* **1987**, *12*, 7342.
(39) Freed, H. F. *J. Phys. A: Math. Gen.* **1985**, *18*, 871.

(40) Sariban, A.; Binder, K. *J. Chem. Phys.* **1987**, *10*, 5859.
(41) Briber, R. M.; Bauer, B. J.; Hammouda, B. *J. Chem. Phys.* **1994**, *101*, 2592.
(42) Brereton, M. G.; Fischer, E. W.; Herkt-Maetzky, Ch. *J. Chem. Phys.* **1987**, *10*, 6144.
(43) Schweizer, K. S. *Macromolecules* **1993**, *26*, 6033.

MA010576O